Acta Cryst. (1986). A**42**, 340-344

The Ewald Energies of Complex Crystals: the 'Biochlorites'

BY J. OLIVES

CRMC2, Campus de Luminy, 13288 Marseille CEDEX 9, France

(*Received* 27 *September* 1985; *accepted* 11 *March* 1986)

Abstract

Calculation of the electrostatic Ewald energies of complex crystals requires much time. For such crystals, two methods, suggested by the methods of Ewald and Bertaut, are proposed to obtain rapid convergence of the series: the 'multi-radii method' and the 'overlapping method'. These methods are applied to the 'biochlorites', complex crystals formed by mixing biotite and chlorite layers. The Ewald energy of 1-1 biochlorite (1 biotite layer-1 chlorite layer) with a value of 181·6 MJ mol^{-1} (eight tetrahedral cations *T* per molecule) is found to be approximately equal to the sum of the energies of biotite: 74·6 MJ mol^{-1} (four *T* per molecule) and chlorite: 107 MJ mol^{-1} (four *T* per molecule). The energy of mixing (of biotite and chlorite layers) is thus nearly equal to 0, which is an indication of the possible stability of biochlorites.

1. The 'biochlorites'

Micas and chlorites are phyllosilicates: their structure is formed by the stacking of unit layers. Two tetrahedral sheets *T*, formed by tetrahedra $(Si, Al)O_4$, and one octahedral sheet *O* form a talc-like layer *T*-*O*-*T*. The mica structure consists of talc-like layers alternating with planes of cations (generally potassium ions). In the chlorite structure, the talc-like layers alternate with brucite-like layers. Interstratified structures with mixed mica and chlorite layers have been observed with transmission electron microscopy of sufficient resolution (Page & Wenk, 1979; Knipe, 1981; Iijima & Zhu, 1982; Olives, Amouric, de Fouquet & Baronnet, 1983; Veblen, 1983; Veblen & Ferry, 1983; Olives & Amouric, 1984; Maresch, Massonne & Czank, 1985; Olives, 1985*b*). They have generally been interpreted as intermediate states which appear during the transformation of mica into chlorite or chlorite into mica. Nevertheless, we have observed biotites and chlorites in a metamorphic rock (phyllite of Brégançon, Maures massif, France), both containing mixed biotite and chlorite layers (Olives, 1985*b*; Fig. 1 of this paper). Since biotites and chlorites were nearly at equilibrium during metamorphism, these mixing structures are probably stable. These biotites and chlorites are in fact biotite-chlorite interstratifications and we call these crystals 'biochlorites'

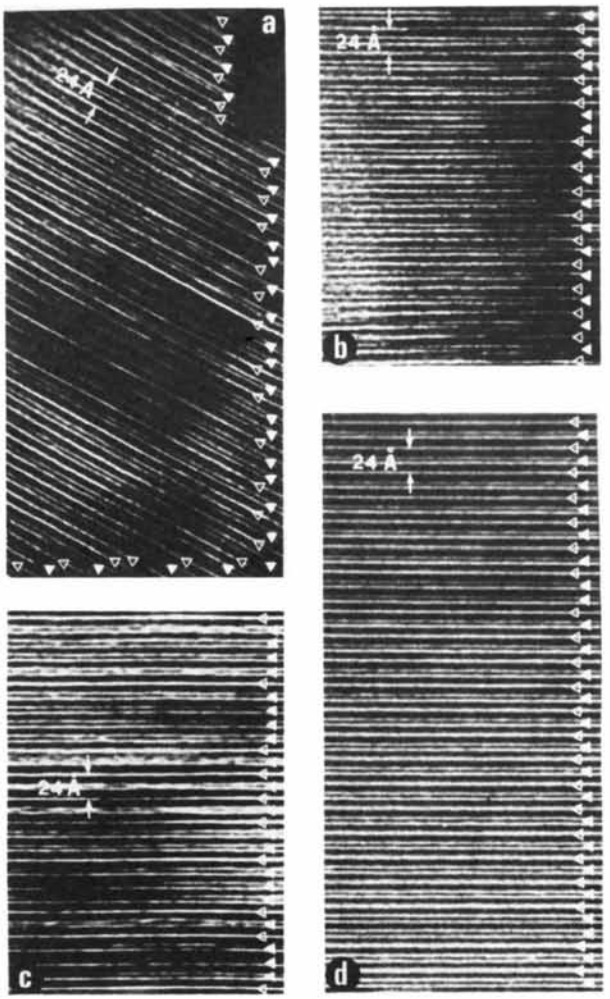

Fig. 1. Images of biochlorites, taken with a transmission electron microscope of high resolution. The triangles, at the sides of the images, indicate the nature of the layers: one empty triangle = one plane of potassium ions (white fringe) ≡ one unit biotite layer; one solid triangle = one brucite-like layer ≡ one chlorite layer; the broad dark bands situated between any two triangles represent the talc-like layers. (*a*) Region of a biotite crystal; disordered *x*-*y* biochlorite (*x* biotite layers-*y* chlorite layers); *x*, *y* = 1 or 2; (*b*) region of a biotite crystal; ordered 1-1 biochlorite, with only one defect consisting of two consecutive chlorite layers; (*c*) region of a chlorite crystal; disordered 1-*x* biochlorite (1 biotite layer-*x* chlorite layers), *x* = 1 to 4; (*d*) region of a chlorite crystal; ordered 1-1 biochlorite (with two defects consisting of two consecutive chlorite layers).

0108-7673/86/050340-05$01.50

for short (Olives, 1985*a*). In the biochlorite structure, a talc-like layer may alternate either with a plane of potassium ions (which gives a unit biotite layer) or with a brucite-like layer (which gives a unit chlorite layer). The sequence of biotite and chlorite layers is generally disordered. Nevertheless, the ordered 1-1 biochlorite (layer sequence: 1 biotite layer-1 chlorite layer) is frequently observed (Olives & Amouric, 1984; Olives, 1985*a*; Maresch *et al.*, 1985; Olives, 1985*b*; Fig. 1 of this paper).

2. Ewald energy calculation methods for complex crystals

2.1. *Introduction*

Let us consider an ionic crystal in which the ions are considered as point charges, and denote by $\mathbf{n}$ the lattice vectors ($\mathbf{n}=n_1\mathbf{a}_1+n_2\mathbf{a}_2+n_3\mathbf{a}_3$; $n_1, n_2, n_3=$ integers), by $\mathbf{s}$ or $\mathbf{t}$ the positions of the ions of the origin cell $\mathbf{n}=\mathbf{0}$, and by q_s the charge of the ion $\mathbf{s}$.

Madelung (1918) calculated the electrostatic lattice potential

$$\Phi(\mathbf{x})=\sum_{\substack{\mathbf{n}\ \mathbf{s}\\ \mathbf{n}+\mathbf{s}\neq\mathbf{x}}}\sum q_s/\|\mathbf{n}+\mathbf{s}-\mathbf{x}\| \qquad (1)$$

for a particular class of crystals (in which the ions may be grouped into electrically neutral parallel straight lines).

Born & Landé (1918) proposed the following expression for E_0 the electrostatic energy per cell:

$$E_0=-\tfrac{1}{2}\sum_{\mathbf{t}} q_t\Phi(\mathbf{t})$$

$$=\tfrac{1}{2}\sum_{\substack{\mathbf{n}\ \mathbf{s}\ \mathbf{t}\\ \mathbf{n}+\mathbf{s}\neq\mathbf{t}}}\sum\sum q_sq_t/\|\mathbf{n}+\mathbf{s}-\mathbf{t}\|. \qquad (2)$$

Ewald (1921) obtained a general formula for the electrostatic potential $\Phi(\mathbf{x})$ (of an arbitrary crystal lattice of point charges). Ewald's formula leads with the help of expression (2) of Born & Landé to a general expression of the electrostatic energy per cell, which we shall call the 'Ewald energy', and denote by E_E (see the next section).

In a recent paper, we have discussed the exact relations which exist between E_E, E_0 and the 'limit electrostatic energy per cell' E (Olives, 1985*c*).

2.2. *Ewald's method*

As noted above, Ewald's formula for the electrostatic potential may be written in the energy form

$$E_E=E_1-E_2+E_3, \qquad (3)$$

with

$$E_1=(1/2\pi V)\sum_{\mathbf{h}\neq\mathbf{0}}|F(\mathbf{h})|^2\exp(-\pi^2\mathbf{h}^2/H^2)/\mathbf{h}^2$$

$$E_2=(H/\pi^{1/2})\sum_{\mathbf{s}} q_s^2$$

$$E_3=\tfrac{1}{2}\sum_{\substack{\mathbf{n}\ \mathbf{s}\ \mathbf{t}\\ \mathbf{n}+\mathbf{s}\neq\mathbf{t}}}\sum\sum(q_sq_t/\|\mathbf{n}+\mathbf{s}-\mathbf{t}\|)$$

$$\times\left[1-(2/\pi^{1/2})\int_0^{\|\mathbf{n}+\mathbf{s}-\mathbf{t}\|H}\exp(-\lambda^2)\,d\lambda\right] \qquad (4)$$

where $V=$ volume of the cell, $\mathbf{h}=$ reciprocal-lattice vectors, $H=$ an arbitrary parameter of inverse-length dimension, and

$$F(\mathbf{h})=\sum_{\mathbf{s}} q_s\exp(2\pi i\mathbf{h}\,.\,\mathbf{s}).$$

2.3. *Bertaut's method*

Bertaut (1952) generalized the preceding result using the same expression (3), where

$$E_1=(1/2\pi V)\sum_{\mathbf{h}\neq\mathbf{0}}|F(\mathbf{h})\varphi(\mathbf{h})|^2/\mathbf{h}^2$$

$$E_2=2\pi\sum_{\mathbf{s}} q_s^2\int_0^{+\infty}up(u)\,du$$

$$=2\sum_{\mathbf{s}} q_s^2\int_0^{+\infty}[\varphi(h)]^2\,dh$$

$$E_3=\tfrac{1}{2}\sum_{\substack{\mathbf{n}\ \mathbf{s}\ \mathbf{t}\\ \mathbf{n}+\mathbf{s}\neq\mathbf{t}}}\sum\sum(q_sq_t/\|\mathbf{n}+\mathbf{s}-\mathbf{t}\|)$$

$$\times\int_{\|\mathbf{n}+\mathbf{s}-\mathbf{t}\|}^{+\infty}4\pi u(u-\|\mathbf{n}+\mathbf{s}-\mathbf{t}\|)p(u)\,du$$

$$=\tfrac{1}{2}\sum_{\substack{\mathbf{n}\ \mathbf{s}\ \mathbf{t}\\ \mathbf{n}+\mathbf{s}\neq\mathbf{t}}}\sum\sum(q_sq_t/\|\mathbf{n}+\mathbf{s}-\mathbf{t}\|)$$

$$\times\{1-(2/\pi)\int_0^{+\infty}[\varphi(h)]^2$$

$$\times[\sin(2\pi h\|\mathbf{n}+\mathbf{s}-\mathbf{t}\|)/h]\,dh\}; \qquad (5)$$

p and φ are defined by

$$p(\mathbf{u})=\int\sigma(\mathbf{x})\sigma(\mathbf{x}+\mathbf{u})\,d\mathbf{x}$$

$$\varphi(\mathbf{h})=\int\sigma(\mathbf{x})\exp(2\pi i\mathbf{h}\,.\,\mathbf{x})\,d\mathbf{x}.$$

$p(\mathbf{u})$ depends only on $u=\|\mathbf{u}\|$ and $\varphi(\mathbf{h})$ on $h=\|\mathbf{h}\|$. The density function σ is non-negative, of spherical symmetry and such that

$$\int\sigma(\mathbf{x})\,d\mathbf{x}=1.$$

Bertaut (1952) used the following particular case:

$$\sigma(\mathbf{x})=\text{constant} \quad \text{if } \|\mathbf{x}\|\leq R$$

$$\sigma(\mathbf{x})=0 \quad \text{if } \|\mathbf{x}\|>R$$

where

$$R\leq d/2, \qquad d=\inf_{\mathbf{n}+\mathbf{s}\neq\mathbf{t}}\|\mathbf{n}+\mathbf{s}-\mathbf{t}\|$$

which leads to

$$E_1 = (1/2\pi V) \sum_{\mathbf{h}\neq\mathbf{0}} |F(\mathbf{h})\varphi(\mathbf{h})|^2/\mathbf{h}^2,$$

$$E_2 = (3/5R) \sum_{\mathbf{s}} q_{\mathbf{s}}^2,$$

$$E_3 = 0, \tag{6}$$

with

$$\varphi(\mathbf{h}) = 3\,(\sin\alpha - \alpha\cos\alpha)/\alpha^3, \qquad \alpha = 2\pi R\|\mathbf{h}\|.$$

2.4. *More appropriate methods for complex crystals*

The advantage of Bertaut's method (6) over Ewald's method is that it avoids calculation of the sum E_3: the inequality condition on the radius R means that the (virtual) charge densities $\mathbf{x} \to q_{\mathbf{s}}\sigma(\mathbf{x}-\mathbf{n}-\mathbf{s})$ do not overlap each other, so that the 'charge overlapping term' E_3 disappears. The best convergence for the sum E_1 is obtained with the maximum value of R, that is, $R = d/2$.

2.4.1. *The 'multi-radii method'*. For complex crystals, in which the distances between neighbouring ions may have very different values, the above condition on R, based on the smallest interatomic distance d, is very constraining. Greater radii may be used (in order to obtain a more rapid convergence of the sum E_1) if we attribute to each ion situated at $\mathbf{n}+\mathbf{s}$ a (virtual) radius $R_{\mathbf{s}}$; the different radii $R_{\mathbf{s}}$ being chosen as great as possible, under the condition that

all the spheres with centre $\mathbf{n}+\mathbf{s}$ and radius $R_{\mathbf{s}}$ do not overlap each other. (7)

Following Bertaut (1952), we introduce the density functions

$$\sigma_{\mathbf{s}}(\mathbf{x}) = 3/4\pi R_{\mathbf{s}}^3 \quad \text{if } \|\mathbf{x}\| \leq R_{\mathbf{s}}$$

$$\sigma_{\mathbf{s}}(\mathbf{x}) = 0 \quad \text{if } \|\mathbf{x}\| > R_{\mathbf{s}}$$

and the (virtual) total charge density

$$\rho(\mathbf{x}) = \sum_{\mathbf{n}}\sum_{\mathbf{s}} q_{\mathbf{s}}\sigma_{\mathbf{s}}(\mathbf{x}-\mathbf{n}-\mathbf{s}).$$

The Fourier transform of ρ can easily be obtained as

$$\mathcal{F}\rho(\mathbf{h}) = \sum_{\mathbf{s}} F_{\mathbf{s}}(\mathbf{h})\varphi_{\mathbf{s}}(\mathbf{h})$$

where

$$F_{\mathbf{s}}(\mathbf{h}) = q_{\mathbf{s}} \exp(2\pi i\mathbf{h}\,.\,\mathbf{s}) \tag{8}$$

and $\varphi_{\mathbf{s}} = \mathcal{F}\sigma_{\mathbf{s}}$, *i.e.*, in this case,

$$\varphi_{\mathbf{s}}(\mathbf{h}) = 3\,(\sin\alpha_{\mathbf{s}} - \alpha_{\mathbf{s}}\cos\alpha_{\mathbf{s}})/\alpha_{\mathbf{s}}^3, \qquad \alpha_{\mathbf{s}} = 2\pi R_{\mathbf{s}}\|\mathbf{h}\|. \tag{9}$$

Then the Fourier transform of the Patterson function P is

$$\mathcal{F}P(\mathbf{h}) = \left|\sum_{\mathbf{s}} F_{\mathbf{s}}(\mathbf{h})\varphi_{\mathbf{s}}(\mathbf{h})\right|^2$$

which leads to the term

$$E_1 = (1/2\pi V) \sum_{\mathbf{h}\neq\mathbf{0}} \left|\sum_{\mathbf{s}} F_{\mathbf{s}}(\mathbf{h})\varphi_{\mathbf{s}}(\mathbf{h})\right|^2/\mathbf{h}^2. \tag{10}$$

On the other hand, by introducing the functions

$$p_{\mathbf{st}}(\mathbf{u}) = \int \sigma_{\mathbf{s}}(\mathbf{x}+\mathbf{u})\sigma_{\mathbf{t}}(\mathbf{x})\,d\mathbf{x},$$

the Patterson function may be written

$$P(\mathbf{u}) = \sum_{\mathbf{s}} q_{\mathbf{s}}^2\, p_{\mathbf{ss}}(\mathbf{u}) + \sum_{\substack{\mathbf{n}\\ \mathbf{n}+\mathbf{s}\neq\mathbf{t}}}\sum_{\mathbf{s}}\sum_{\mathbf{t}} q_{\mathbf{s}}q_{\mathbf{t}}p_{\mathbf{st}}(\mathbf{u}-\mathbf{n}-\mathbf{s}+\mathbf{t}),$$

which leads to

$$E_2 = \tfrac{1}{2}\sum_{\mathbf{s}} q_{\mathbf{s}}^2 \int [p_{\mathbf{ss}}(\mathbf{u})/\|\mathbf{u}\|]\,d\mathbf{u}$$

$$= \tfrac{3}{5}\sum_{\mathbf{s}} q_{\mathbf{s}}^2/R_{\mathbf{s}} \tag{11}$$

and

$$E_3 = 0 \tag{12}$$

owing to the non-overlapping condition (7).

The result of this method, expressed by (3), together with (10), (11) and (12), generalizes Bertaut's result (6).

2.4.2. *The 'overlapping method'*. Another way to obtain a rapid convergence is to consider greater values of R in Bertaut's method: in this case ($R > d/2$) there is overlapping of the spheres (of radius R) centred at $\mathbf{n}+\mathbf{s}$, and the sum of the series E_3 given by (5) must be calculated. This may easily and exactly be achieved in our case, because this sum is finite. Indeed, with the value

$$p(u) = (3/8\pi R^6)(2R^3 - 3R^2u/2 + u^3/8) \quad \text{if } u \leq 2R$$

$$p(u) = 0 \quad \text{if } u > 2R$$

given by Bertaut (1952), we may calculate the integral:

$$4\pi \int_{\|\mathbf{n}+\mathbf{s}-\mathbf{t}\|}^{+\infty} u(u - \|\mathbf{n}+\mathbf{s}-\mathbf{t}\|)p(u)\,du$$

$$= 1 - (6/5)\|\mathbf{n}+\mathbf{s}-\mathbf{t}\|/R + (1/2)(\|\mathbf{n}+\mathbf{s}-\mathbf{t}\|/R)^3 - (3/16)(\|\mathbf{n}+\mathbf{s}-\mathbf{t}\|/R)^4 + (1/160) \times (\|\mathbf{n}+\mathbf{s}-\mathbf{t}\|/R)^6,$$

and we obtain

$$E_3 = \frac{1}{2R}\sum_{\substack{\mathbf{n}\\ \mathbf{n}+\mathbf{s}\neq\mathbf{t}\\ \|\mathbf{n}+\mathbf{s}-\mathbf{t}\|<2R}}\sum_{\mathbf{s}}\sum_{\mathbf{t}} q_{\mathbf{s}}q_{\mathbf{t}} \times \left(\frac{1}{x_{\mathbf{nst}}} - \frac{6}{5} + \frac{1}{2}x_{\mathbf{nst}}^2 - \frac{3}{16}x_{\mathbf{nst}}^3 + \frac{1}{160}x_{\mathbf{nst}}^5\right) \tag{13}$$

where

$$x_{\mathbf{nst}} = \|\mathbf{n}+\mathbf{s}-\mathbf{t}\|/R.$$

The result of this method is thus expressed by (3), where E_1 and E_2 are given by (6) and E_3 by (13). As R is increased, the series E_1 converges more rapidly, but, at the same time, the number of terms in the finite sum E_3 increases.

3. The Ewald energies of the biochlorites

In order to study the stability of biochlorites, we have calculated the lattice energies of biotite, chlorite and 1-1 biochlorite. A first approximation to the lattice energy is the electrostatic Ewald energy of the ionic lattice (the ions being considered as point charges). This energy has been calculated by the preceding methods (§ 2). We have used the atomic coordinates given by Rayner (1974) for biotite and by Joswig, Fuess, Rothbauer, Takeuchi & Mason (1980) for chlorite. The basal parameters of biotite have been slightly modified in order to match those of chlorite. From these two structures, we have then built the 1-1 biochlorite structure: the unit biotite layer and the unit chlorite layer have been considered as limited by two successive octahedral cation planes (of the talc-like layers); the stacking of the biotite and chlorite layers is such that all the 'talc-staggers' (stagger between the two tetrahedral sheets T of a talc layer T-O-T) are identical. The ionic charges for biotite are those of phlogopite, and the same charges are used for the talc-like layers of chlorite (which determines the cation charges in the brucite-like layers). We obtain the following Ewald energies: 74·6 MJ mol^{-1} (for four tetrahedral cations T per molecule) for biotite [very similar to the values of Giese (1975) and Jenkins & Hartman (1979)]; 107 MJ mol^{-1} (four T per molecule) for chlorite; 181·6 MJ mol^{-1} (eight T per molecule) for 1-1 biochlorite (Olives, 1985*a*, *b*). We note that the lattice energy of 1-1 biochlorite is approximately equal to the sum of the lattice energies of biotite and chlorite. In other words, the energy needed to mix biotite and chlorite layers taken from a pure biotite and a pure chlorite crystal is nearly equal to 0. Approximately the same energy is needed to form a biochlorite, or to form separately a pure biotite crystal and a pure chlorite crystal. This result is an indication of the possible stability of biochlorites.

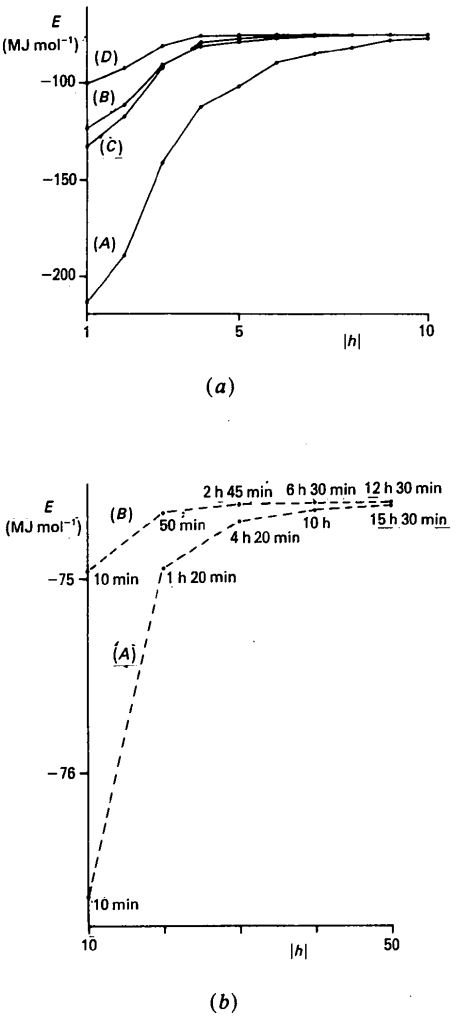

Fig. 2. Ewald energy of biotite calculated up to $|h| = \sup(|h_1|, |h_2|, |h_3|)$; (*A*) Bertaut's method (6); (*B*) 'multi-radii method'; (*C*) and (*D*) 'overlapping method', with $R = 0{\cdot}75$ Å for (*C*), and $R = 1$ Å for (*D*). (*a*) $|h| = 1$ to 10. The calculation time for $|h| = 10$ is about 10 min for all the methods. Curves (*B*) and (*C*) cross each other between $|h| = 3$ and 4. (*b*) $|h| = 10$ to 50. The calculation times are indicated near each point.

4. Comparison of the different calculation methods

Biochlorites are complex crystals containing a great number of ions per cell (44 ions per cell for biotite, 72 for chlorite, 116 for 1-1 biochlorite). In the simple case of NaCl, the calculation of the partial sum of the series E_1 up to $|h| = \sup(|h_1|, |h_2|, |h_3|) = 5$ gives the value of the energy with a relative precision of 7×10^{-4}; and this requires less than one second of calculation time. However, in the case of biotite (the most simple biochlorite), the calculation must be

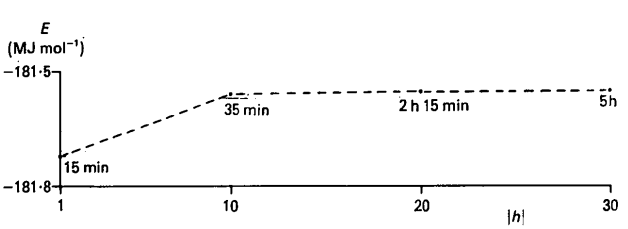

Fig. 3. Ewald energy of 1-1 biochlorite calculated up to $|h| = \sup(|h_1|, |h_2|, |h_3|)$, for $|h| = 1$ to 30; 'overlapping method' with $R = 4$ Å. The calculation times are indicated near each point.

performed up to $|h|=38$ with Bertaut's method (6), in order to obtain the same relative precision; and this requires 8 h 45 min of calculation time. All the calculations were made on a 16-bit minicomputer (DEC PDP11/45).

In the biochlorites, the smallest interatomic distance d is the O-H distance of about 1 Å; thus, the radius R of Bertaut's method (6) must be about 0·5 Å. Because all other O-cation distances are greater than 1 Å, a more rapid convergence is obtained with the 'multi-radii method' (of § 2.4.1), as shown in Fig. 2 for the case of biotite. With the 'overlapping method' (§ 2.4.2) we may choose $R>0{\cdot}5$ Å; the convergence is similar to that of the 'multi-radii method' if $R=0{\cdot}75$ Å, and it is more rapid if $R>0{\cdot}75$ Å(Fig. 2*a*). This is also illustrated in Fig. 3, in the case of 1-1 biochlorite: with $R=4$ Å, the series E_1 converges very rapidly and the finite sum E_3 requires only 15 min of calculation time. Higher values of R give a better convergence for E_1, but a longer calculation time for E_3.

References

BERTAUT, F. (1952). *J. Phys. Radium*, **13**, 499-505.
BORN, M. & LANDÉ, A. (1918). *Verh. Dtsch. Phys. Ges.* **20**, 210-216.
EWALD, P. P. (1921). *Ann. Phys. (Leipzig)*, **64**, 253-287.
GIESE, R. F. (1975). *Z. Kristallogr.* **141**, 138-144.
IIJIMA, S. & ZHU, J. (1982). *Am. Mineral.* **67**, 1195-1205.
JENKINS, H. D. B. & HARTMAN, P. (1979). *Philos. Trans. R. Soc. London Ser. A*, **293**, 169-208.
JOSWIG, W., FUESS, H., ROTHBAUER, R., TAKEUCHI, Y. & MASON, A. (1980). *Am. Mineral.* **65**, 349-352.
KNIPE, R. J. (1981). *Tectonophysics*, **78**, 249-272.
MADELUNG, E. (1918). *Phys. Z.* **19**, 524-532.
MARESCH, W. V., MASSONNE, H.-J. & CZANK, M. (1985). *Neues Jahrb. Mineral. Abh.* **152**, 79-100.
OLIVES, J. (1985*a*). *Terra Cognita*, **5**, 226.
OLIVES, J. (1985*b*). *Bull. Minéral.* **108**, 635-641.
OLIVES, J. (1985*c*). *J. Phys. (Paris) Lett.* **46**, 1143-1149.
OLIVES, J. & AMOURIC, M. (1984). *Am. Mineral.* **69**, 869-871.
OLIVES, J., AMOURIC, M., DE FOUQUET, C. & BARONNET, A. (1983). *Am. Mineral.* **68**, 754-758.
PAGE, R. H. & WENK, H. R. (1979). *Geology*, **7**, 393-397.
RAYNER, J. H. (1974). *Mineral. Mag.* **39**, 850-856.
VEBLEN, D. R. (1983). *Am. Mineral.* **68**, 566-580.
VEBLEN, D. R. & FERRY, J. M. (1983). *Am. Mineral.* **68**, 1160-1168.

Acta Cryst. (1986). A**42**, 344-348

Comparison of an *Umweganregung* Pattern, Measured on an Automatic Single-Crystal Diffractometer, With Calculated Patterns

BY ELISABETH ROSSMANITH

Mineralogisch-Petrographisches Institut der Universität Hamburg, Grindelallee 48, *D*-2000 *Hamburg* 13, *Federal Republic of Germany*

(*Received* 20 *August* 1985; *accepted* 24 *March* 1985)

Abstract

The ψ scan of the forbidden 003 reflection of Zn, measured with an automatic single-crystal diffractometer, using Cu $K\alpha$ radiation, is compared with the calculated and plotted *Umweganregung* pattern for Cu $K\alpha_1$ and Cu $K\alpha_2$ radiation. The intensities of the *Umweganregung* peaks are calculated on the basis of the kinematical theory. When the Lorentz factors for both scans involved in the measurement (the θ scan and the ψ scan) are taken into account, excellent agreement between measured and calculated intensities is obtained. The width of the *Umweganregung* peaks can be explained by replacing the reciprocal-lattice points by spheres in reciprocal space.

Introduction

In the last few years interest in weak high-order reflections measured with X-rays of short wavelength has increased in structure analysis. Multiple diffraction systematically increases the weak intensities and falsifies the intensity data sets. The influence of the simultaneous reflections on weak intensities must therefore be investigated thoroughly, using the experimental arrangement of the automatic single-crystal diffractometer employed in structure analysis.

Since Renninger (1937) carried out a systematic investigation into the multiple diffraction phenomenon in the ψ-scanning pattern of the 222 reflection of diamond, many papers on this topic have been published. An extensive bibliography of this subject is given by Post (1975, 1976) and in papers cited therein. Recently the computer program *UMWEG* was published by the author (Rossmanith, 1985); this program is based mainly on the geometrical considerations of Cole, Chambers & Dunn (1962).

Simultaneous diffraction occurs when three or more reciprocal-lattice points lie simultaneously on

0108-7673/86/050344-05$01.50